

Received August 23, 2019, accepted September 7, 2019, date of publication September 13, 2019,
date of current version September 30, 2019.

Digital Object Identifier 10.1109/ACCESS.2019.2941278

UAV-Aided Wireless Powered Communication Networks: Trajectory Optimization and Resource Allocation for Minimum Throughput Maximization

JUNHEE PARK^{ID¹}, HOON LEE^{ID²}, (Member, IEEE), SUBIN EOM^{ID¹},
AND INKYU LEE^{ID¹}, (Fellow, IEEE)

¹School of Electrical Engineering, Korea University, Seoul 02841, South Korea

²Department of Information and Communications Engineering, Pukyong National University, Busan 48513, South Korea

Corresponding author: Inkyu Lee (inkyu@korea.ac.kr)

This work was supported by the National Research Foundation through the Ministry of Science, ICT, and Future Planning (MSIP), Korean Government, under Grant 2017R1A2B3012316.

ABSTRACT This paper investigates wireless powered communication network (WPCN) systems aided by unmanned aerial vehicle (UAV) where a UAV-mounted access point (AP) serves multiple energy-constrained ground terminals (GTs). Specifically, the UAVs first transmit the wireless energy transfer (WET) signals to charge the GTs in the downlink. Then, by utilizing the harvested energy, the GTs send their wireless information transmission (WIT) signals to the UAVs in the uplink. In this paper, depending on the operations of the UAVs, we consider two different scenarios, namely integrated and separated UAV WPCNs. First, in the integrated system, a UAV acts as a hybrid AP in which both energy transfer and information reception are performed at a single UAV. In contrast, for the separated UAV WPCN, we consider two UAVs each of which behaves as an information AP and an energy AP independently, and thus the information decoding and the energy transfer are separately processed at two different UAVs. In each system, we formulate two optimization problems taking into account a linear energy harvesting (EH) model and a practical non-linear model. To maximize the minimum throughput of the GTs, we jointly optimize the trajectories of the UAVs, the uplink power control, and the time resource allocation for the WET and the WIT. Since the formulated problems are non-convex, in the linear EH model-based system, we apply the concave-convex procedure by deriving appropriate convex bounds for non-convex constraints and identify the suboptimal solution for the problem by a proposed iterative algorithm. In the non-linear model-based system, we propose another algorithm to obtain an efficient solution by adopting the successive convex approximation method with the alternating optimization framework. Simulation results demonstrate the efficiency and the performance of the proposed algorithms compared to conventional schemes.

INDEX TERMS UAV communication, wireless powered communication networks, trajectory optimization.

I. INTRODUCTION

Recently, unmanned aerial vehicles (UAVs) have been adopted in many applications such as cargo transport and military operations [2], [3], and thus deploying the UAV has

The associate editor coordinating the review of this manuscript and approving it for publication was Qinghua Guo.

drawn huge attentions in the field of wireless communications [4]–[15]. Compared to traditional networks where APs are fixed on the ground, wireless communication networks employing a UAV-mounted access point (AP) exhibit deployment flexibility and cost-efficiency. Moreover, the mobility of the UAV can provide an opportunity for the networks to enhance the system capacity.

In [4]–[6], UAV-enabled relaying channels were studied where UAVs act as mobile relays which forward the information from sources to destinations located on the ground. For the UAV relay networks, deployment and direction control problems were investigated in [4], and the work in [5] minimized the network outage probability when the UAV trajectory is given as a circular path. The authors in [6] solved the throughput maximization problem by optimizing the relay and the source transmit power allocation along with the trajectory of UAV relay. In addition, UAVs have been employed as mobile base stations in various wireless networks [7]–[11]. The mobile base station placement problems were investigated in [7] and [8] for maximizing the overall wireless coverage. In [9], analytical expressions of the optimal UAV height were derived to optimize the air-to-ground links outage probability. The authors in [10] focused on the mathematical energy consumption modeling for UAVs, and proposed trajectory optimization methods for maximizing the energy efficiency of a UAV. Also, the trajectories of multiple UAVs were examined in [11] to maximize the minimum throughput performance of multiple ground terminals (GTs). Moreover, UAV-aided caching and mobile cloud computing systems were researched in [12] and [13], respectively.

In the meantime, radio frequency (RF) signal-based energy harvesting (EH) have been considered as promising techniques for prolonging the battery lifetime of wireless devices [16]–[25]. By utilizing wireless information transmission (WIT) and wireless energy transfer (WET), the RF-based EH techniques have been investigated for traditional wireless networks, and recent studies have examined wireless powered communication networks (WPCN) protocols [22]–[25].

Particularly, in the downlink WET phase of the WPCN, a hybrid access point (H-AP) transfers wireless energy via the RF signals to battery-limited devices. In the successive uplink WIT phase, by exploiting the harvested energy, the devices transmit information signals to the H-AP. In [22], throughput maximization problems were introduced for the WPCN by optimizing the time resource allocated to users under the harvest-then-transmit protocol. The authors in [23] proposed the multi-antenna energy beamforming and time allocation algorithms to maximize the minimum throughput performance. The sum-rate maximization problems with a full-duplex H-AP were investigated in [24] for orthogonal frequency division multiplexing, and the precoding methods for the multiple-input multiple-output WPCN was provided in [25]. Note that these works were limited to a fixed H-AP setup, and thus it would cause the ‘doubly near-far’ problem [22], which is inherent to the downlink and uplink signal attenuation dominated by the distance between the H-AP and the devices. Recently, there have been many works combining mobile vehicle techniques with the WET [26]–[34]. For the magnetic resonant based WET, [26]–[29] considered wireless charging vehicles which travel the networks to supply power to wireless sensors. However, due to short charging coverage of the magnetic resonance technique, the vehicles should

stay quite a while to transfer energy to nearby sensors and thus it would not be easy to transfer enough energy to sensors distributed in a wide area. To overcome this limitation, the authors in [30] adopted the RF-based WET methods to UAV-aided WPCN where a UAV flies towards a GT to transmit the RF energy signal and receive uplink data. However, only a single GT case was considered in [30] where the UAV trajectory is fixed to a line segment without optimizing the traveling path. Although the UAV-enabled WET networks were examined in [31]–[34], they did not take into account the communication procedures among UAVs and GTs.

In this paper, we investigate the UAV-aided WPCN where UAVs with arbitrary trajectories serve multiple energy-constrained GTs which do not have embedded energy sources. Such a scenario prevails in wireless sensor networks and internet of things (IoT) environment. Depending on the roles of the UAVs, we classify the UAV WPCN into two categories: integrated UAV and separated UAV WPCNs. First, in the integrated UAV WPCN, a single UAV behaves as an H-AP which broadcasts the RF energy signal to the GTs in the downlink WET phase and decodes the information from the GTs in the uplink WIT phase. In contrast, in the separated UAV WPCN, the WET and WIT operations are assigned to two different UAVs separately. To be specific, we could employ a dedicated WET UAV without requiring communication circuits for the uplink data decoding, which results in a cost-effective UAV design. Also, by dividing these two operations, the system performance can be further improved.

In both systems, we adopt a time division multiple access (TDMA) based harvest-then-transmit protocol in [22] where the WET of the UAVs and the WIT at the GTs are processed over orthogonal time resources. Also, we consider both linear and non-linear models for the RF EH circuits. First, the UAV-aided WPCN is analyzed based on a linear EH model where the harvested power of the EH circuit is linearly related to the input RF power. Next, to deal with the non-linear behavior of realistic rectifying circuits, a practical EH model, which characterizes the saturation and sensitivity effects of the rectifier, is additionally investigated. Although the non-linear property of the practical EH circuit is important in the UAV-aided WPCN, it has not yet been adequately studied in the literature due to the nonconvexity of the UAV movement features.

The UAV-aided WPCN has been investigated in recent literatures [1], [30]. In our previous work [1], only the integrated WPCN system was considered under the ideal linear EH model assumption. In this scenario, the trajectory optimization problem was solved by fixing the time resource allocation variable. On the contrary, in this paper, we will address a joint optimization of the trajectory, the uplink power, and the time durations both for the integrated and separated WPCN systems. In addition, we take the practical non-linear EH model into account. Hence, the system model and a solution of [1] can be regarded as a special case of this work. Also, compared to [30] where the trajectory of the UAV is restricted

to a straight line, our systems consider a general travelling path optimization problem without any constraints on the UAV trajectory.

As the problems are non-convex, we propose iterative algorithms to obtain a solution by applying various optimization methods. In the linear EH model-based system, we employ the concave-convex procedure (CCCP) method [35], [36] which successively solves approximated convex problems of the original problem to jointly optimize the trajectory of the UAVs, the uplink power of the GTs, and the time resource allocation solutions. In contrast, for the non-linear EH model-based system, we first jointly optimize the trajectory of the UAVs and the uplink power of the GTs with given time allocation based on the successive convex approximation (SCA) framework [37], and then update the time resource allocation solution with linear programming (LP) by fixing other variables. The convergence of the proposed algorithms is then mathematically proved. From numerical results, we demonstrate that the proposed algorithms substantially improve the performance of the UAV WPCN compared to conventional schemes and can be implemented in practical scenarios as an effective off-line scheduling scheme as in [31].

The remainder of this paper is organized as follows: Section II describes a system model of the UAV-aided WPCN and formulates the minimum throughput optimization problems. In Sections III and IV, we present algorithms based on the linear and non-linear EH models, respectively. Simulation results for the proposed algorithms are described in Section V to demonstrate the performance enhancement over conventional baseline schemes. The paper concludes in Section VI.

In this paper, we employ normal and boldface lowercase letters to represent scalars and column vectors, respectively. For the transpose operation as $(\cdot)^T$, and \mathbb{R}^n stands for the Euclidean space of dimension n . Also, $|\cdot|$ and $\|\cdot\|$ represent the magnitude and the Euclidean norm, respectively.

II. SYSTEM MODEL

As shown in Figure 1, we consider a UAV-aided WPCN where UAVs collect the data of K GTs in the uplink. The UAVs and GTs are equipped with a single antenna. It is assumed that the UAVs have constant power sources [6], [8], whereas no embedded energy supplies are available for

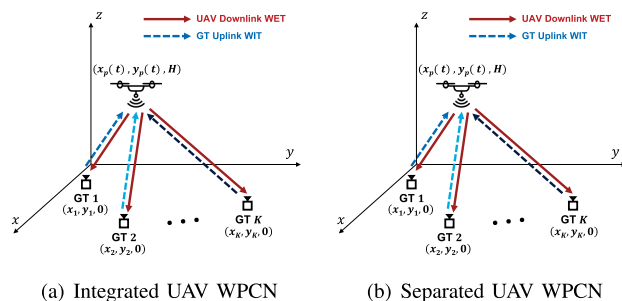


FIGURE 1. Schematic diagrams of UAV-aided WPCNs.

the GTs. The UAVs wirelessly charge the GTs through down-link channels. By utilizing the harvested energy from the UAV, the GTs transmit their information in the uplink. In this work, a UAV network is considered where the UAVs support the uplink communication of the GTs for a pre-determined time period T [15], [38]. The time period T is regarded as a design parameter which depends on the battery capacity of the UAVs and the network delay-throughput performance [15]. We assume that the flying altitude of the UAVs is fixed to H and their speed is upper-bounded by v_{\max} , whereas all the GTs are fixed at given locations.

Depending on the operations of the UAVs, we classify the UAV-aided WPCN into two categories. First, in the integrated UAV WPCN illustrated in Figure 1(a), a single UAV transmits energy and collects data of the GTs. Thus, the UAV in the integrated UAV WPCN acts as an H-AP in the conventional WPCN [22]. Second, in the separated UAV WPCN in Figure 1(b), the WET and the WIT are independently performed at two different UAVs. Therefore, each UAV in the separated system is dedicated to the energy transferring (ET) or the information decoding (ID). In the following, we first present the system models for both UAV WPCNs based on the linear EH model.

A. LINEAR EH MODEL-BASED SYSTEM

1) INTEGRATED UAV WPCN

In the integrated UAV WPCN, let us define $\mathbf{p}(t) = [x_p(t), y_p(t)]^T$ as the UAV location at a certain time $t \in [0, T]$, and it is assumed that the location of GT $k \in \mathcal{K} \triangleq \{1, \dots, K\}$, denoted as $\mathbf{u}_k = [x_k, y_k]^T$, is priorly informed to the UAV. For convenience of analysis, we divide the total time period T into N equal-length time slots as in [11], where N is chosen to be large enough so that the distance between the UAV and the GTs are unchanged within each time slot.

Therefore, a sequence of the UAV locations $\{\mathbf{p}[n]\}$ at each time slot $n \in \mathcal{N} \triangleq \{1, \dots, N\}$ is given as

$$\mathbf{p}[n] \triangleq \mathbf{p}(n\delta_N) = [x_p(n\delta_N), y_p(n\delta_N)]^T, \quad (1)$$

where $\delta_N \triangleq T/N$ denotes the length of each slot. Since we consider the discrete time trajectory $\{\mathbf{p}[n]\}$, the maximum speed constraint can be written as

$$\|\mathbf{p}[n] - \mathbf{p}[n-1]\| \leq \delta_N v_{\max}, \quad \text{for } n \in \hat{\mathcal{N}} \triangleq \{2, \dots, N\}. \quad (2)$$

For the air-to-ground channel between the UAV and the GTs, we adopt the deterministic propagation model which assumes the log-distance path-loss links without the Doppler effect [6], [10], [13]. Note that this model can provide reference performance for practical fading channels. Then, the average channel gain $G_k[n]$ between GT $k \in \mathcal{K}$ and the UAV at time slot $n \in \mathcal{N}$ is given by

$$G_k[n] = \frac{g_0}{(\|\mathbf{p}[n] - \mathbf{u}_k\|^2 + H^2)^{\gamma/2}}, \quad (3)$$

where g_0 and $\gamma \geq 2$ denote the reference channel gain at a distance of 1 meter and the path-loss exponent, respectively.

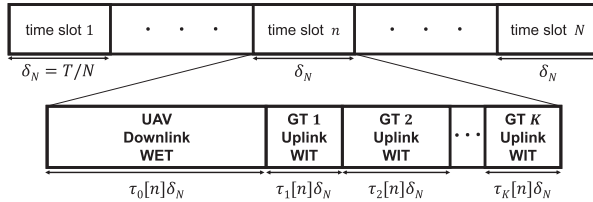


FIGURE 2. Protocol structure for UAV-aided WPCN.

Next, we describe the transmission protocol for the UAV WPCN. As shown in Figure 2, we divide each time slot n into $K + 1$ subslots, where the first subslot of duration $\tau_0[n]\delta_N$ is allocated to the dedicated downlink WET and the remaining k -th subslot of duration $\tau_k[n]\delta_N$ for $k \in \mathcal{K}$ is assigned to the uplink WIT of GT k . Here, $\tau_k[n]$, which is an optimization variable to be determined, accounts for the time duration at the k -th subslot in time slot n . Then, we have the following constraints on the time resource allocation optimization variable $\tau_k[n]$ as

$$0 \leq \tau_k[n] \leq 1, \quad \text{for } n \in \mathcal{N} \text{ and } k \in \check{\mathcal{K}}, \quad (4)$$

$$\sum_{k=0}^K \tau_k[n] \leq 1, \quad \text{for } n \in \mathcal{N}, \quad (5)$$

where $\check{\mathcal{K}} \triangleq \mathcal{K} \cup \{0\}$.

Now, the WIT and the WET process of the integrated UAV WPCN is explained. During the first subslot of each time slot n , i.e., $\tau_0[n]\delta_N$, the energy signals are broadcasted by the UAV with the transmission power P^{DL} . Note that the downlink power P^{DL} is negligible compared to the mechanical power consumption of commercial UAVs in general [39], and does not affect the operation duration of the UAVs. Then, in the linear EH model, the harvested energy $E_k^L[n]$ of GT $k \in \mathcal{K}$ at time slot $n \in \mathcal{N}$ can be expressed as

$$E_k^L[n] \triangleq \tau_0[n]\delta_N \zeta_k G_k[n] P^{\text{DL}} = \frac{\tau_0[n]\delta_N \zeta_k g_0 P^{\text{DL}}}{(\|\mathbf{p}[n] - \mathbf{u}_k\|^2 + H^2)^{\gamma/2}}, \quad (6)$$

where $\zeta_k \in (0, 1]$ stands for the energy conversion efficiency of GT k reflecting hardware impairment of practical RF EH circuits. For simplicity, it is assumed that the energy harvesting efficiency of all the GTs is identical, i.e., $\zeta_k = \zeta$ for $k \in \mathcal{K}$. Due to the processing delay of the EH circuit, the GTs may not be able to utilize the harvested energy $E_k^L[n]$ immediately at time slot n . Hence, GT k only can use $E_k^L[n]$ at the future time slots $n+1, n+2, \dots, N$. Then, the available energy of GT k at time slot n can be written as

$$\tilde{E}_k[n] = \sum_{i=1}^{n-1} E_k^L[i] - \sum_{i=1}^{n-1} \tau_k[i]\delta_N P_k^{\text{UL}}[i], \quad (7)$$

where $P_k^{\text{UL}}[n]$ represents the uplink transmit power of GT k at time slot n . Note that the first summation in (7) indicates the cumulative harvested energy while the second one accounts for the consumed energy at GT k during the past time slots for $i = 1, 2, \dots, n-1$. As a result, the uplink power constraint

for GT k at time slot n is given as

$$\tau_k[n]\delta_N P_k^{\text{UL}}[n] \leq \tilde{E}_k[n], \quad \text{for } n \in \hat{\mathcal{N}} \text{ and } k \in \mathcal{K}. \quad (8)$$

Without loss of the generality, it is assumed that the system bandwidth is normalized to the unity. Then, the instantaneous throughput $R_k[n]$ [bps/Hz] of GT k at time slot n can be obtained as

$$\begin{aligned} R_k[n] &\triangleq \log_2 \left(1 + \frac{\eta_k G_k[n] P_k^{\text{UL}}[n]}{\sigma^2} \right) \\ &= \log_2 \left(1 + \frac{g_0 \eta_k}{\sigma^2} \frac{P_k^{\text{UL}}[n]}{(\|\mathbf{p}[n] - \mathbf{u}_k\|^2 + H^2)^{\gamma/2}} \right), \end{aligned} \quad (9)$$

where σ^2 is the noise variance and $\eta_k \in (0, 1]$ denotes a portion of the stored energy used for the uplink information transmission at GT k . Note that the remaining $(1 - \eta_k)$ portion of the remaining energy is consumed for the on-board processing such as data sensing, circuit operations, and information collection. For simplicity, we assume that $\eta_k = \eta$ for $k \in \mathcal{K}$. Then, for the time period T , the average throughput R_k of GT $k \in \mathcal{K}$ can be written by

$$\begin{aligned} R_k &\triangleq \frac{1}{T} \delta_N \sum_{n=2}^N \tau_k[n] R_k[n] \\ &= \sum_{n=2}^N \frac{\tau_k[n]}{N} \log_2 \left(1 + \frac{\frac{g_0 \eta}{\sigma^2} P_k^{\text{UL}}[n]}{(\|\mathbf{p}[n] - \mathbf{u}_k\|^2 + H^2)^{\gamma/2}} \right). \end{aligned} \quad (10)$$

In this paper, we aim to maximize the minimum average throughput among the GTs by jointly optimizing the trajectory of the UAV $\{\mathbf{p}[n]\}$, the uplink power of the GTs $\{P_k^{\text{UL}}[n]\}$, and the time resource allocation variables $\{\tau_k[n]\}$. We introduce an optimization variable R_{\min} for reflecting the minimum throughput among the GTs, i.e., $R_k \geq R_{\min}$. By using the epigraph reformulation technique [40], the maximization task of the minimum throughput performance can be formulated as

$$\begin{aligned} (\text{P1}) \quad &\max_{R_{\min}, \{P_k^{\text{UL}}[n]\}, \{\mathbf{p}[n]\}, \{\tau_k[n]\}} R_{\min} \\ &\text{s.t. } R_k \geq R_{\min}, \quad \text{for } k \in \mathcal{K}, \end{aligned} \quad (11)$$

$$\sum_{i=2}^n \tau_k[i] P_k^{\text{UL}}[i] \leq \frac{1}{\delta_N} \sum_{i=1}^{n-1} E_k^L[i], \quad \text{for } n \in \hat{\mathcal{N}} \text{ and } k \in \mathcal{K}, \quad (12)$$

$$\|\mathbf{p}[n] - \mathbf{p}[n-1]\| \leq \delta_N v_{\max}, \quad \text{for } n \in \hat{\mathcal{N}}, \quad (13)$$

$$\mathbf{p}[0] = \mathbf{p}[N], \quad (14)$$

$$\begin{aligned} 0 \leq P_k^{\text{UL}}[n] \leq P_{\max}^{\text{UL}}, \quad \text{for } n \in \mathcal{N} \text{ and } k \in \mathcal{K}, \\ (4) - (5), \end{aligned} \quad (15)$$

where the energy for uplink transmission is constrained by (12) which is derived from (8), and (14) represents the periodicity of the trajectory so that the UAV has to return to the starting place after a period of time T [11].¹ The constraint

¹Depending on the application, one may want to determine the initial location and the final location of the UAV in advance. In this case, we can simply add constraints on $\mathbf{p}[0]$ and $\mathbf{p}[N]$ and discard the constraint in (14).

in (15) indicates the maximum allowable uplink power at each time slot. It can be checked that (P1) is a non-convex problem due to the constraints (11) and (12), and therefore it is not straightforward to determine the globally optimal solution.

Remark 1: With the constraint in (14), the UAV is guaranteed to periodically drop by its starting position $\mathbf{p}[0]$ after the time period T . The position $\mathbf{p}[0]$, or equivalently, $\mathbf{p}[N]$, can be considered as the location of the UAV control center which is responsible for checking the conditions of the UAVs and the overall network procedure [11]. Based on the UAV swapping strategy [38]², we can build continuous WPCN supports for the GTs by deploying several backup UAVs.

2) SEPARATED UAV WPCN

In the separated UAV WPCN, we design the trajectories of two different UAVs, i.e., ID UAV and ET UAV. Let us define $\mathbf{p}_I[n] \in \mathbb{R}^2$ and $\mathbf{p}_E[n] \in \mathbb{R}^2$ as the position of the ET UAV and the ID UAV at time slot n , respectively. Similar to the integrated UAV WPCN, we adopt the TDMA protocol in Figure 2. Then, the uplink energy constraint of GT k at time slot n and the average throughput of GT k $R_{k,S}$ can be respectively expressed as

$$\begin{aligned} & \tau_k[n] P_k^{\text{UL}}[n] \\ & \leq \sum_{i=1}^{n-1} \left(\frac{\tau_0[i] \xi_k g_0 P^{\text{DL}}}{(\|\mathbf{p}_E[i] - \mathbf{u}_k\|^2 + H_E^2)^{\gamma/2}} - \tau_k[i] P_k^{\text{UL}}[i] \right), \quad (16) \end{aligned}$$

$$R_{k,S} \triangleq \sum_{n=2}^N \frac{\tau_k[n]}{N} \log_2 \left(1 + \frac{\frac{g_0 \eta}{\sigma^2} P_k^{\text{UL}}[n]}{(\|\mathbf{p}_I[n] - \mathbf{u}_k\|^2 + H_I^2)^{\gamma/2}} \right), \quad (17)$$

where H_I and H_E stand for the flight altitude of the ID UAV and the ET UAV, respectively.

Thus, the minimum throughput maximization problem for the separated UAV WPCN is given

$$\begin{aligned} & (\text{P2}) \max_{\substack{R_{\min}, \{P_k^{\text{UL}}[n]\}, \{\mathbf{p}_I[n]\}, \\ \{\mathbf{p}_E[n]\}, \{\tau_k[n]\}}} R_{\min} \\ & \text{s.t. } R_{k,S} \geq R_{\min}, \quad \text{for } k \in \mathcal{K}, \quad (18) \end{aligned}$$

$$\sum_{i=2}^n \tau_k[i] P_k^{\text{UL}}[i] \leq \sum_{i=1}^{n-1} \frac{\tau_0[i] g_0 \xi_k P^{\text{DL}}}{(\|\mathbf{p}_E[i] - \mathbf{u}_k\|^2 + H_E^2)^{\gamma/2}}, \\ \text{for } n \in \hat{\mathcal{N}} \text{ and } k \in \mathcal{K}, \quad (19)$$

$$\|\mathbf{p}_x[n] - \mathbf{p}_x[n-1]\| \leq \delta_N v_{\max}^x, \\ \text{for } x \in \{I, E\} \text{ and } n \in \hat{\mathcal{N}}, \quad (20)$$

$$\mathbf{p}_x[0] = \mathbf{p}_x[N], \quad \text{for } x \in \{I, E\}, \quad (21)$$

$$(4) - (5), (15),$$

where v_{\max}^I and v_{\max}^E represent the maximum speed of the ID UAV and the ET UAV, respectively. This problem is also non-convex due to the constraints (18) and (19).

²In this scenario, several backup UAVs can be prepared at the control center so that UAVs with low batteries can be replaced by new ones with fully-charged batteries [38]. Thus, we can handle the limited battery issue of the UAVs since it is sufficient for the UAVs to operate within the time duration.

B. NON-LINEAR EH MODEL-BASED SYSTEM

For the non-linear EH system, we adopt a sigmoid function-based model [21], and the harvested energy $E_k^{\text{NL}}[n]$ is given by

$$E_k^{\text{NL}}[n] \triangleq \frac{\tau_0[n] \delta_N}{\alpha} \left(\frac{M(1+\alpha)}{1+\alpha \exp\left(-\frac{-\beta g_0 P^{\text{DL}}}{(\|\mathbf{p}[n] - \mathbf{u}_k\|^2 + H^2)^{\gamma/2}}\right)} - M \right), \quad (22)$$

where M denotes a constant representing the maximum harvested power at a GT when the EH circuit is saturated, and α and β are constants determined by the circuit specifications. With this model, similar to (P1), we can formulate another optimization problem for the integrated UAV WPCN with the non-linear EH model as

$$\begin{aligned} & (\text{P1-NL}) \max_{\substack{R_{\min}, \{P_k^{\text{UL}}[n]\}, \{\mathbf{p}[n]\}, \{\tau_k[n]\}}} R_{\min} \\ & \text{s.t. } R_k \geq R_{\min}, \quad \text{for } k \in \mathcal{K}, \quad (23) \end{aligned}$$

$$\sum_{i=2}^n \tau_k[i] P_k^{\text{UL}}[i] \leq \frac{1}{\delta_N} \sum_{i=1}^{n-1} E_k^{\text{NL}}[i],$$

$$\text{for } n \in \hat{\mathcal{N}} \text{ and } k \in \mathcal{K}, \quad (24)$$

$$(4) - (5), (13) - (15).$$

Note that (P1-NL) is also non-convex due to the constraints in (23) and (24). Furthermore, since the practical non-linear EH circuits involve the saturation issue of input-output power represented by $E_k^{\text{NL}}[n]$ in (24), (P1-NL) needs to be addressed by a different approach compared to (P1). As a result, the algorithm for (P1) cannot be applied to (P1-NL) directly. In the following sections, we present efficient approaches for solving (P1), (P1-NL), and (P2).³

III. PROPOSED SOLUTION FOR LINEAR EH MODEL

In this section, we propose iterative optimization algorithms for the linear EH model problems (P1) and (P2). To this end, we employ the CCCP framework which finds an efficient solution for the UAV trajectories $\{\mathbf{p}[n]\}$ (or $\{\mathbf{p}_I[n]\}$ and $\{\mathbf{p}_E[n]\}$), the uplink power $\{P_k^{\text{UL}}[n]\}$, and the time resource allocation $\{\tau_k[n]\}$ by iteratively addressing convex approximation problems of the original non-convex ones. We first discuss the integrated UAV WPCN (P1), and then it is followed by the solution approach for the separated system (P2).

A. INTEGRATED UAV WPCN

To make (P1) tractable, let us first apply a change of variable $\{\varepsilon_k[n]\}$ such that $\varepsilon_k[n] \geq 0$ and $\varepsilon_k[n]^2 = \tau_k[n] P_k^{\text{UL}}[n]$ for $k \in \mathcal{K}$ and $n \in \mathcal{N}$. Then, (P1) can be recast to

$$\max_{\substack{R_{\min}, \{\varepsilon_k[n]\}, \{\mathbf{p}[n]\}, \{\tau_k[n]\}}} R_{\min} \quad (25)$$

$$\text{s.t. } \sum_{n=2}^N \frac{\tau_k[n]}{N} \log_2 \left(1 + \frac{\frac{g_0 \eta}{\sigma^2} \varepsilon_k[n]^2 / \tau_k[n]}{(\|\mathbf{p}[n] - \mathbf{u}_k\|^2 + H^2)^{\gamma/2}} \right) \\ \geq R_{\min}, \quad \text{for } k \in \mathcal{K}, \quad (26)$$

³Similar to (P1-NL), we can also formulate the non-linear EH model-based optimization problem in the separated UAV WPCN but the problem is omitted for brevity.

$$\sum_{i=2}^n \varepsilon_k[i]^2 \leq \sum_{i=1}^{n-1} \tau_0[i] \frac{g_0 \zeta_k P_{\text{DL}}}{(\|\mathbf{p}[i] - \mathbf{u}_k\|^2 + H^2)^{\gamma/2}},$$

for $n \in \hat{\mathcal{N}}$ and $k \in \mathcal{K}$, (27)

$$\varepsilon_k[n]^2 \leq P_{\max}^{\text{UL}} \tau_k[n], \text{ for } n \in \mathcal{N} \text{ and } k \in \mathcal{K},$$

(4) - (5), (13) - (14).

Still, the problem in (25) is non-convex in general due to the constraints in (26) and (27). To tackle this difficulty, we introduce an auxiliary variable $\{z_k[n]\}$ such that $(\|\mathbf{p}[n] - \mathbf{u}_k\|^2 + H^2)^{\gamma/2} \leq z_k[n]$ for $k \in \mathcal{K}$ and $n \in \mathcal{N}$. Applying the change of variables $\tau_0[n] = \omega[n]^2$ for $n \in \mathcal{N}$, the left-hand-side (LHS) of (26) and the right-hand-side (RHS) of (27) are respectively lower-bounded by

$$\begin{aligned} & \sum_{n=2}^N \frac{\tau_k[n]}{N} \log_2 \left(1 + \frac{\frac{g_0 \eta}{\sigma^2} \varepsilon_k[n]^2 / \tau_k[n]}{(\|\mathbf{p}[n] - \mathbf{u}_k\|^2 + H^2)^{\gamma/2}} \right) \\ & \geq \sum_{n=2}^N \frac{\tau_k[n]}{N} \log_2 \left(1 + \frac{\frac{g_0 \eta}{\sigma^2} \varepsilon_k[n]^2}{\tau_k[n] z_k[n]} \right), \end{aligned} \quad (29)$$

$$\sum_{i=1}^{n-1} \tau_0[i] \frac{g_0 \zeta P_{\text{DL}}}{(\|\mathbf{p}[i] - \mathbf{u}_k\|^2 + H^2)^{\gamma/2}} \geq \sum_{i=1}^{n-1} g_0 \zeta P_{\text{DL}} \frac{\omega[i]^2}{z_k[i]}. \quad (30)$$

Based on (29) and (30), in the following proposition, we can construct an equivalent problem for (25).

Proposition 1: The optimal solution for the problem in (25) can be obtained by solving the following optimization problem:

$$\begin{aligned} (\text{P1.1}) \quad & \max_{\substack{R_{\min}, \{\varepsilon_k[n]\}, \{\mathbf{p}[n]\}, \\ \{\tau_k[n]\}, \{z_k[n]\}, \{\omega[n]\} \{X_k[n]\}}} R_{\min} \\ & \text{s.t. } \frac{1}{N} \sum_{n=2}^N \tau_k[n] \log_2 \left(1 + \frac{\frac{g_0 \eta}{\sigma^2} X_k[n]}{\tau_k[n]} \right) \geq R_{\min}, \end{aligned} \quad \text{for } k \in \mathcal{K}, \quad (31)$$

$$\sum_{i=2}^n \varepsilon_k[i]^2 \leq \sum_{i=1}^{n-1} g_0 \zeta P_{\text{DL}} \frac{\omega[i]^2}{z_k[i]},$$

for $n \in \hat{\mathcal{N}}$ and $k \in \mathcal{K}$, (32)

$$X_k[n] \leq \frac{\varepsilon_k[n]^2}{z_k[n]}, \quad \text{for } n \in \mathcal{N} \text{ and } k \in \mathcal{K} \quad (33)$$

$$\|\mathbf{p}[n] - \mathbf{u}_k\|^2 + H^2 \leq z_k[n]^{\frac{2}{\gamma}},$$

for $n \in \mathcal{N}$ and $k \in \mathcal{K}$,

(4) - (5), (13) - (14), (28).

Proof: First, let R_{\min}^* and \tilde{R}_{\min} denote the optimal value of problem (25) and (P1.1), respectively. Then it can easily be checked that $R_{\min}^* \geq \tilde{R}_{\min}$, where the equality holds when $z_k[n]^{\frac{2}{\gamma}} = \|\mathbf{p}[n] - \mathbf{u}_k\|^2 + H^2$ and $X_k[n] = \frac{\varepsilon_k[n]^2}{z_k[n]}$, $\forall n$ and $\forall k$. Next, by contradiction, we will prove that the optimum of (P1.1) can be attained when $z_k[n]^{\frac{2}{\gamma}} = \|\mathbf{p}[n] - \mathbf{u}_k\|^2 + H^2$ and $X_k[n] = \frac{\varepsilon_k[n]^2}{z_k[n]}$. Suppose that there exists at least one $X_k[n]$ or $z_k[n]$ such that at the optimum of (P1.1), the equalities

in (33) or (34) does not hold and denote a set of such k as $\mathcal{K}' \subset \mathcal{K}$. If the equality holds in (31) for $k' \in \mathcal{K}'$ in this case, the minimum throughput \tilde{R}_{\min} can be improved by reducing $z_{k'}[n]$ and increasing $X_{k'}[n]$ so that constraints (33) and (34) hold with equality. This contradicts the assumption that there are $X_k[n]$ or $z_k[n]$ such that the equalities in (33) or (34) does not hold at the optimum of (P1.1). Even if the equality does not hold in (31) for k' at the optimum, increasing $z_{k'}[n]$ does not affect the minimum throughput \tilde{R}_{\min} . Therefore, for all these cases, we can always find the optimal $z_k[n]$ and $X_k[n]$ for (P1.1) satisfying $z_k[n]^{\frac{2}{\gamma}} = \|\mathbf{p}[n] - \mathbf{u}_k\|^2 + H^2$ and $X_k[n] = \frac{\varepsilon_k[n]^2}{z_k[n]}$. As a result, by solving (P1.1), the optimal solution of (25) can be attained equivalently.⁴ ■

(P1.1) is still non-convex in general due to constraint in (32) and (33). Thus, we provide the CCCP [35] approach to address (P1.1). First, we consider the uplink available energy constraint in (32). Since the RHS of (32) is a jointly convex function over $z_k[n]$ and $\omega[n]$, by using a first-order Taylor approximation at $z_k[n] = \hat{z}_k[n]$ and $\omega[n] = \hat{\omega}[n]$, we can derive a lower bound of the RHS of (32) as

$$\begin{aligned} & \sum_{i=1}^{n-1} g_0 \zeta P_{\text{DL}} \frac{\omega[i]^2}{z_k[i]} \\ & \geq \sum_{i=1}^{n-1} \frac{g_0 \zeta P_{\text{DL}} \hat{\omega}[i]}{\hat{z}_k[i]} \left(2\omega[i] - \hat{\omega}[i] - \frac{\hat{\omega}[i](z_k[i] - \hat{z}_k[i])}{\hat{z}_k[i]} \right) \\ & \triangleq \sum_{i=1}^{n-1} E_{k,\text{LB}}^L[i](\omega[i], z_k[i] | \hat{\omega}[i], \hat{z}_k[i]). \end{aligned} \quad (35)$$

Note that $E_{k,\text{LB}}^L[n](\omega[n], z_k[n] | \hat{\omega}[n], \hat{z}_k[n])$ is an affine function with respect to $\omega[n]$ and $z_k[n]$, and gives a tight lower bound in which equality holds at $\omega[n] = \hat{\omega}[n]$ and $\hat{z}_k[n] = z_k[n]$. In a similar manner, the RHS of the auxiliary constraint in (33), which is a jointly convex function with respect to $\varepsilon_k[n]$ and $z_k[n]$, can be lower-bounded by

$$\begin{aligned} \frac{\varepsilon_k[n]^2}{z_k[n]} & \geq \frac{\hat{\varepsilon}_k[n]^2}{\hat{z}_k[n]} + \frac{2\hat{\varepsilon}_k[n]}{\hat{z}_k[n]} (\varepsilon_k[n] - \hat{\varepsilon}_k[n]) \\ & \quad - \frac{\hat{\varepsilon}_k[n]^2}{\hat{z}_k[n]^2} (z_k[n] - \hat{z}_k[n]) \\ & \triangleq A_k[n](\varepsilon_k[n], z_k[n] | \hat{\varepsilon}_k[n], \hat{z}_k[n]). \end{aligned} \quad (36)$$

With (35) and (36) at hand, a convex approximation of (P1.1) with given $\hat{z}_k[n]$, $\hat{\varepsilon}_k[n]$, and $\hat{\omega}[n]$ can be formulated as

$$\begin{aligned} (\text{P1.1A}) \quad & \max_{\substack{R_{\min}, \{\varepsilon_k[n]\}, \{\mathbf{p}[n]\}, \\ \{\tau_k[n]\}, \{z_k[n]\}, \{\omega[n]\} \{X_k[n]\}}} R_{\min} \\ & \text{s.t. } \sum_{i=2}^n \varepsilon_k[i]^2 \leq \sum_{i=1}^{n-1} E_{k,\text{LB}}^L[i](\omega[i], z_k[i] | \hat{\omega}[i], \hat{z}_k[i]), \end{aligned} \quad \text{for } n \in \hat{\mathcal{N}} \text{ and } k \in \mathcal{K}, \quad (37)$$

⁴Based on Proposition 1, the quality-of-service (QoS) constraint can be considered in a similar way to equation (31).

$$\begin{aligned} X_k[n] \leq A_k[n](\varepsilon_k[n], z_k[n] | \hat{\varepsilon}_k[n], \hat{z}_k[n]), \\ \text{for } n \in \mathcal{N} \text{ and } k \in \mathcal{K}, \\ (4) - (5), (13) - (14), (28) - (31), (34). \end{aligned} \quad (38)$$

(P1.1A) can be solved by existing convex solvers, e.g., CVX [41]. Since the feasible region of (P1.1A) is a subset of that of the original problem (P1.1), we can always obtain a lower bound solution for problem (P1.1) from its approximation (P1.1A). As a result, a solution for (P1.1) can be calculated by solving a series of the convex problem (P1.1A) at each iteration. At the q -th iteration of the CCCP algorithm, we compute the solution $\hat{z}_k^{(q)}[n]$, $\hat{\varepsilon}_k^{(q)}[n]$ and $\hat{\omega}^{(q)}[n]$ of (P1.1A) by setting $\hat{z}_k[n] = z_k^{(q-1)}[n]$, $\hat{\varepsilon}_k[n] = \varepsilon_k^{(q-1)}[n]$ and $\hat{\omega}[n] = \omega^{(q-1)}[n]$, where $z_k^{(q)}[n]$, $\varepsilon_k^{(q)}[n]$ and $\omega^{(q)}[n]$ are the solution determined at the q -th iteration. It has been proved that this CCCP method converges to at least a stationary point [35]. One algorithm for solving (P1) is summarized in Algorithm 1 below.

Algorithm 1 Proposed Algorithm for (P1) With the Linear EH Model

Initialize $z_k^{(q)}[n]$, $\varepsilon_k^{(q)}[n]$ and $\omega^{(q)}[n]$, $\forall n$ and $\forall k$, and set $q = 0$.

Repeat

- Update $q \leftarrow q + 1$.
- Set $\hat{z}_k[n] = z_k^{(q-1)}[n]$, $\hat{\varepsilon}_k[n] = \varepsilon_k^{(q-1)}[n]$ and $\hat{\omega}[n] = \omega^{(q-1)}[n]$, $\forall n$ and $\forall k$.
- Solve (P1.1A) by using the CVX.
- Until convergence
- Set $\mathbf{p}^*[n] = \mathbf{p}^{(q)}[n]$, $P_k^{\text{UL}*}[n] = \frac{\varepsilon_k^{(q)}[n]^2}{\tau_k[n]}$, $\tau_0^*[n] = \omega^{(q)}[n]^2$, and $\tau_k^*[n] = \tau_k^{(q)}[n]$, $\forall n$ and $\forall k$.

Once Algorithm 1 converges, we can retrieve the corresponding solution of the original problem (P1) as

$$\mathbf{p}^*[n] = \mathbf{p}^{(q)}[n], \quad \text{for } n \in \mathcal{N}, \quad (39)$$

$$\tau_0^*[n] = \omega^{(q)}[n]^2 \quad \text{and} \quad \tau_k^*[n] = \tau_k^{(q)}[n], \quad \text{for } n \in \mathcal{N} \text{ and } k \in \mathcal{K}, \quad (40)$$

$$P_k^{\text{UL}*}[n] = \begin{cases} \frac{\varepsilon_k^{(q)}[n]^2}{\tau_k[n]}, & \text{for } \tau_k[n] \neq 0, \\ 0, & \text{for } \tau_k[n] = 0 \end{cases}, \quad \text{for } n \in \hat{\mathcal{N}} \text{ and } k \in \mathcal{K}. \quad (41)$$

With the location of the GTs at hand, Algorithm 1 is an off-line procedure performed at the UAV control center whose computing power is typically sufficient for executing iterative calculation processes. Then, a solution can be informed to the UAVs and the GTs in advance, and the optimized time durations are utilized for off-line scheduling among the UAVs and the GTs. For more reliable communication between the UAVs and the GTs, control and non-payload communication links can be established in addition to the data communication links [2].

B. SEPARATED UAV WPCN

In this subsection, we present an efficient algorithm for (P2) in the separated UAV WPCN. Similar to the integrated system, an efficient solution for the trajectories $\{\mathbf{p}_I[n]\}$ and $\{\mathbf{p}_E[n]\}$, the uplink power $\{P_k^{\text{UL}}[n]\}$, and time resource allocation solution $\{\tau_k[n]\}$ can be obtained by iteratively solving a approximated problem of (P2).

To solve the non-convex problem (P2), similar to (P1.1), we introduce new auxiliary variables $\{z_k^I[n]\}$ and $\{z_k^E[n]\}$ such that $(\|\mathbf{p}_I[n] - \mathbf{u}_k\|^2 + H_I^2)^{\gamma/2} \leq z_k^I[n]$ and $(\|\mathbf{p}_E[n] - \mathbf{u}_k\|^2 + H_E^2)^{\gamma/2} \leq z_k^E[n]$ for $k \in \mathcal{K}$ and $n \in \mathcal{N}$. Then, (P2) can be reformulated as

$$\begin{aligned} (\text{P2.1}) \quad & \max_{R_{\min}, \{\varepsilon_k[n]\}, \{\mathbf{p}_I[n]\}, \{\mathbf{p}_E[n]\}, \\ & \{\tau_k[n]\}, \{z_k[n]\}, \{\omega[n]\}, \{Y_k[n]\}} R_{\min} \\ & \text{s.t.} \frac{1}{N} \sum_{n=2}^N \tau_k[n] \log_2 \left(1 + \frac{\frac{g_0 \eta}{\sigma^2} Y_k[n]}{\tau_k[n]} \right) \geq R_{\min}, \end{aligned} \quad (42)$$

$$\sum_{i=2}^n \varepsilon_k[i]^2 \leq \sum_{i=1}^{n-1} g_0 \xi P^{\text{DL}} \frac{\omega[i]^2}{z_k^E[i]}, \quad \text{for } n \in \hat{\mathcal{N}} \text{ and } k \in \mathcal{K}, \quad (43)$$

$$Y_k[n] \leq \frac{\varepsilon_k[n]^2}{z_k^I[n]}, \quad \text{for } n \in \mathcal{N} \text{ and } k \in \mathcal{K}, \quad (44)$$

$$\|\mathbf{p}_I[n] - \mathbf{u}_k\|^2 \leq z_k^I[n]^{\frac{2}{\gamma}}, \quad \text{for } n \in \mathcal{N} \text{ and } k \in \mathcal{K}, \quad (45)$$

$$\|\mathbf{p}_E[n] - \mathbf{u}_k\|^2 \leq z_k^E[n]^{\frac{2}{\gamma}}, \quad \text{for } n \in \mathcal{N} \text{ and } k \in \mathcal{K}, \quad (46)$$

(4) - (5), (20) - (21), (28), where $\{\varepsilon_k[n]\}$ and $\{\omega[n]\}$ are auxiliary variables defined in Section III-A. The equivalence between problem (P2) and (P2.1) can be easily verified by a similar approach in Proposition 1.

One can check that (P2.1) the non-convex constraints (43) and (44), which are given by the difference of two convex functions, can be handled by the CCCP method [35]. Thus, at each iteration of the CCCP algorithm, we address the following approximated convex problem as

$$\begin{aligned} (\text{P2.1A}) \quad & \max_{R_{\min}, \{\varepsilon_k[n]\}, \{\mathbf{p}_I[n]\}, \{\mathbf{p}_E[n]\}, \\ & \{\tau_k[n]\}, \{z_k[n]\}, \{\omega[n]\}, \{Y_k[n]\}} R_{\min} \\ & \text{s.t.} \sum_{i=2}^n \varepsilon_k[i]^2 \leq \sum_{i=1}^{n-1} E_{k,\text{LB}}^L[i](\omega[i], z_k^E[i] | \hat{\omega}[i], \hat{z}_k^E[i]), \end{aligned} \quad (47)$$

$$Y_k[n] \leq A_k[n](\varepsilon_k[n], z_k^I[n] | \hat{\varepsilon}_k[n], \hat{z}_k^I[n]), \quad \text{for } n \in \mathcal{N} \text{ and } k \in \mathcal{K}, \quad (48)$$

$$(4) - (5), (20) - (21), (28), (42), (45) - (46),$$

where the approximations in (47) and (48) are obtained from (35) and (36), respectively. Therefore, we can reach a stationary point for (P2.1) by iteratively solving (P2.1A) with $\hat{z}_k^I[n] = z_k^{I(q)}[n]$, $\hat{z}_k^E[n] = z_k^{E(q)}[n]$, $\hat{\varepsilon}_k[n] = \varepsilon_k^{(q)}[n]$ and $\hat{\omega}[n] = \omega^{(q)}[n]$ for $n \in \mathcal{N}$ and $k \in \mathcal{K}$, whose convergence

has been shown in [35]. The overall procedure is similar to that for (P1.1) and thus omitted here for brevity.

IV. PROPOSED SOLUTION FOR NON-LINEAR EH MODEL

So far, we have investigated efficient optimization procedures under the ideal assumption with the linear EH model. Although the linear EH model is analytically simple, it cannot capture the non-linear property of real-world EH circuits at the GTs. This is important for the UAV-aided WPCN systems since the input power to the rectifier may change fast due to the mobility of the UAVs. In this section, we propose a solution for the practical non-linear EH model [42], [43]. Due to the non-linear nature of the input-output EH relationship, it is not trivial to tackle (P1-NL) via the algorithms developed for the linear EH model. Therefore, we employ the alternating optimization method which first obtains a solution for the trajectory $\{\mathbf{p}[n]\}$ and the uplink power $\{P_k^{\text{UL}}[n]\}$ with given time resource allocation $\{\tau_k[n]\}$, and then computes $\{\tau_k[n]\}$ by fixing $\{\mathbf{p}[n]\}$ and $\{P_k^{\text{UL}}[n]\}$.

A. JOINT TRAJECTORY AND UPLINK POWER OPTIMIZATION

For a given time resource allocation $\{\tau_k[n]\}$, (P1-NL) can be recast to

$$\begin{aligned} & \max_{R_{\min}, \{P_k^{\text{UL}}[n]\}, \{\mathbf{p}[n]\}} R_{\min} \\ & \text{s.t. } (13) - (15), (23) - (24). \end{aligned} \quad (49)$$

Problem (49) is again non-convex due to the constraints in (23) and (24). To tackle this difficulty, by using the auxiliary variables $\{z_k[n]\}$ introduced in Section III-A, we can respectively lower-bound the LHS of (23) and the RHS of (24) as

$$\begin{aligned} & \sum_{n=2}^N \frac{\tau_k[n]}{N} \log_2 \left(1 + \frac{\frac{g_0 \eta}{\sigma^2} P_k^{\text{UL}}[n]}{(\|\mathbf{p}[n] - \mathbf{u}_k\|^2 + H^2)^{\gamma/2}} \right) \\ & \geq \sum_{n=2}^N \frac{\tau_k[n]}{N} \log_2 \left(1 + \frac{\frac{g_0 \eta}{\sigma^2} P_k^{\text{UL}}[n]}{z_k[n]} \right), \end{aligned} \quad (50)$$

$$\begin{aligned} & \tau_0[n] \frac{M}{\alpha} \left(\frac{1+\alpha}{1+\alpha \exp(-\frac{\beta g_0 P^{\text{DL}}}{(\|\mathbf{p}[n] - \mathbf{u}_k\|^2 + H^2)^{\gamma/2}})} - 1 \right) \\ & \geq \tau_0[n] \frac{M}{\alpha} \left(\frac{1+\alpha}{1+\alpha \exp(-\frac{\beta g_0 P^{\text{DL}}}{z_k[n]})} - 1 \right), \end{aligned} \quad (51)$$

where equalities hold when $\|\mathbf{p}[n] - \mathbf{u}_k\|^2 + H^2 = z_k[n]^{\frac{2}{\gamma}}$. For these bounds, an equivalent problem of (49) can be constructed from the following proposition.

Proposition 2: The optimal solution for the problem (49) can be obtained by solving the following optimization problem:

$$\begin{aligned} & (\text{P1.2}) \quad \max_{R_{\min}, \{P_k^{\text{UL}}[n]\}, \{\mathbf{p}[n]\}, \{z_k[n]\}} R_{\min} \\ & \text{s.t. } \frac{1}{N} \sum_{n=2}^N \tau_k[n] \log_2 \left(1 + \frac{\frac{g_0 \eta}{\sigma^2} P_k^{\text{UL}}[n]}{z_k[n]} \right) \geq R_{\min}, \\ & \quad \text{for } k \in \mathcal{K}, \end{aligned} \quad (52)$$

$$\begin{aligned} & \sum_{i=2}^n \tau_k[i] P_k^{\text{UL}}[i] \\ & \leq \sum_{i=1}^{n-1} \frac{\tau_0[n] M}{\alpha} \left(\frac{1+\alpha}{1+\alpha \exp(-\frac{\beta g_0 P^{\text{DL}}}{z_k[n]})} - 1 \right), \\ & \quad \text{for } n \in \hat{\mathcal{N}} \text{ and } k \in \mathcal{K}, \end{aligned} \quad (53)$$

(13) - (15), (34).

Proof: The proof is similar to that of Proposition 1 and thus omitted for brevity. ■

We provide the SCA approach [37] to address the non-convexity of (P1.2) by reformulating the non-convex constraints into the approximated convex ones, which had not been investigated in the existing literature related to the linear EH model-based UAV-aided WET system [31]–[34] yet. First, we consider the minimum throughput constraint in (52). By applying a first-order Taylor expansion at $z_k[n] = \hat{z}_k[n]$, a concave surrogate function for the LHS of (52) can be derived as

$$\begin{aligned} & \log_2 \left(1 + \frac{\frac{g_0 \eta}{\sigma^2} P_k^{\text{UL}}[n]}{z_k[n]} \right) \\ & \geq \log_2 \left(1 + \frac{z_k[n] + \frac{g_0 \eta}{\sigma^2} P_k^{\text{UL}}[n]}{\hat{z}_k[n]} \right) - \frac{z_k[n] - \hat{z}_k[n]}{\hat{z}_k[n] \ln 2} \\ & \triangleq R_{k,\text{LB}}[n](z_k[n], P_k^{\text{UL}}[n] | \hat{z}_k[n]). \end{aligned} \quad (54)$$

Note that $R_{k,\text{LB}}[n](z_k[n], P_k^{\text{UL}}[n] | \hat{z}_k[n])$ is jointly concave for $z_k[n]$ and $P_k^{\text{UL}}[n]$, and provides a tight lower bound where the inequality in (54) reduces to equality when $\hat{z}_k[n] = z_k[n]$. Next, for the RHS of constraint (53), which is neither convex nor concave on $z_k[n]$, we construct another concave surrogate function $E_{k,\text{LB}}^{\text{NL}}[n](z_k[n] | \hat{z}_k[n])$ by the following proposition.

Proposition 3: For given $z_k[n] = \hat{z}_k[n]$, a concave surrogate function of the RHS of (53) can be constructed as

$$\begin{aligned} & E_{k,\text{LB}}^{\text{NL}}[n](z_k[n] | \hat{z}_k[n]) \\ & = \tau_0[n] M \left(\frac{1 - \exp(-\hat{Z}_k[n])}{1 + \alpha \exp(-\hat{Z}_k[n])} \right. \\ & \quad \left. + \frac{(1+\alpha)\hat{Z}_k[n]^2 \exp(-\hat{Z}_k[n])(z_k[n] - \hat{z}_k[n])}{\beta g_0 P^{\text{DL}}(1+\alpha \exp(-\hat{Z}_k[n]))^2} \right) \\ & \quad + \frac{U_m}{2}(z_k[n] - \hat{z}_k[n])^2, \end{aligned} \quad (55)$$

where $\hat{Z}_k[n] \triangleq \frac{\beta g_0 P^{\text{DL}}}{\hat{z}_k[n]}$ and $U_m \triangleq \min_{z_k[n] \in \mathbb{R}} U(z_k[n])$.

Proof: Please refer to Appendix A. ■

Using (54) and (55), we can approximate (P1.2) into a convex problem for given $\hat{z}_k[n]$ as

$$\begin{aligned} & (\text{P1.2A}) \quad \max_{R_{\min}, \{P_k^{\text{UL}}[n]\}, \{\mathbf{p}[n]\}, \{z_k[n]\}} R_{\min} \\ & \text{s.t. } \frac{1}{N} \sum_{n=2}^N \tau_k[n] R_{k,\text{LB}}[n](z_k[n], P_k^{\text{UL}}[n] | \hat{z}_k[n]) \geq R_{\min}, \\ & \quad \text{for } k \in \mathcal{K}, \end{aligned} \quad (56)$$

$$\sum_{i=2}^n \tau_k[i] P_k^{\text{UL}}[i] \leq \frac{1}{\delta_N} \sum_{i=1}^{n-1} E_{k,\text{LB}}^{\text{NL}}[i] (z_k[i] | \hat{z}_k[i]),$$

for $n \in \hat{\mathcal{N}}$ and $k \in \mathcal{K}$, (57)

(13) - (15), (34).

Thanks to the convexity of (P1.2A), it can be efficiently solved by existing convex solvers. As a result, a solution for (P1.2) can be calculated by iteratively solving (P1.2A) based on the SCA procedure. At the i -th iteration of the SCA algorithm, (P1.2A) is computed by setting $\hat{z}_k[n] = z_k^{(i-1)}[n]$, where $z_k^{(i)}[n]$ is the solution determined at the i -th iteration.

B. TIME RESOURCE ALLOCATION

Now, we identify a solution for the time resource allocation $\{\tau_k[n]\}$ for given $\{\mathbf{p}[n]\}$ and $\{P_k^{\text{UL}}[n]\}$. The problem is written as

$$\begin{aligned} (\text{P1.3}) \quad & \max_{R_{\min}, \{\tau_k[n]\}} R_{\min} \\ & \text{s.t. (4) - (5), (23) - (24).} \end{aligned}$$

It can be shown that (P1.3) is a convex LP, which can be optimally solved by the standard LP optimization tools.

Algorithm 2 Proposed Algorithm for (P1-NL) with the Non-Linear EH Model

Initialize $\tau_k^{(q)}[n]$ and $\mathbf{p}^{(q)}[n]$, $\forall n$ and $\forall k$, and set $q = 0$.
 Repeat
 Update $q \leftarrow q + 1$, $i \leftarrow 0$.
 Set $z_k^{(q,i)}[n] = \|\mathbf{p}^{(q-1)}[n] - \mathbf{u}_k\|^2$, $\forall n$ and $\forall k$.
 Repeat
 Set $\hat{z}_k[n] = z_k^{(q,i)}[n]$, $\forall n$ and $\forall k$.
 Solve (P1.2A) for given $\{\tau_k^{(q-1)}[n]\}$.
 Update $i \leftarrow i + 1$.
 Until convergence
 Update $\mathbf{p}^{(q)}[n] = \mathbf{p}^{(q,i)}[n]$ and $P_k^{\text{UL}(q)}[n] = P_k^{\text{UL}(q,i)}[n]$.
 Compute $R_{\min}^{(q)}$ and $\{\tau_k^{(q)}[n]\}$ from (P1.3).
 Until $R_{\min}^{(q)}$ converges

Finally, the solution of (P1-NL) can be obtained by employing the alternating optimization framework and the overall process is given in Algorithm 2. In this algorithm, (P1.2) and (P1.3) are iteratively solved by fixing $\{\tau_k[n]\}$ and $\{\mathbf{p}[n], P_k^{\text{UL}}[n]\}$, respectively. To be specific, at the q -th iteration, we first successively solve (P1.2A) for given $\{\tau_k^{(q-1)}[n]\}$ based on the SCA until the objective value converges. Note that we denote the solution obtained at the i -th iteration of the SCA method as $\{\mathbf{p}^{(q,i)}[n], P_k^{\text{UL}(q,i)}[n], z_k^{(q,i)}[n]\}$. Then, the solution of (P1.3) is computed for given $\{\mathbf{p}^{(q)}[n], P_k^{\text{UL}(q)}[n]\}$, and this procedure is repeated until convergence.

Now, we verify the convergence of Algorithm 2. Let us define $\tilde{R}_{\min}^{(q)}$ and $R_{\min}^{(q)}$ as the objective value from the SCA procedure for (P1.2) and the optimal value of (P1.3) at the q -th iteration, respectively. Then, it is obvious that

$R_{\min}^{(q)} \leq \tilde{R}_{\min}^{(q+1)}$ since the SCA algorithm monotonically increases the objective value of (P1.2A) with respect to the iteration index i . Also, due to the fact that $R_{\min}^{(q+1)}$ is the global optimal value of (P1.3) for given $\{\mathbf{p}^{(q+1)}[n]\}$ and $\{P_k^{\text{UL}(q+1)}[n]\}$, it follows $\tilde{R}_{\min}^{(q+1)} \leq R_{\min}^{(q+1)}$. As a result, we have

$$R_{\min}^{(q)} \leq \tilde{R}_{\min}^{(q+1)} \leq R_{\min}^{(q+1)},$$

which implies that $R_{\min}^{(q)}$ is non-decreasing with respect to the iteration index q . Because the minimum throughput R_{\min} is upper-bounded by a certain value, Algorithm 2 is guaranteed to converge. Similar to Algorithm 1, a solution of Algorithm 2 computed by the control center can also be informed to the UAVs before the operation. Also, since the approximated problems (P1.1A) and (P1.2A) are convex, Algorithms 1 and 2 have polynomial time computational complexity and take at most $\mathcal{O}(1/\epsilon)$ iterations to converge where ϵ represents the error tolerance [37], [41]. Thus, the proposed algorithms can be efficiently applied to the UAV WPCNs in practice.

V. SIMULATION RESULTS

In this section, we evaluate the performance of the proposed algorithms by numerical results which are implemented with the convex solver CVX [41]. Unless stated otherwise, the downlink transmission power at the UAVs and the maximum allowable uplink power at the GTs are equal to $P^{\text{DL}} = 40$ dBm and $P^{\text{UL}}_{\max} = -20$ dBm, respectively. Also, ζ and η are fixed as $\zeta = 0.2$ and $\eta = 0.9$, respectively. We set the reference channel gain g_0 to $g_0 = -30$ dB, and the path-loss exponent and the noise variance are given by $\gamma = 2$ and $\sigma^2 = -90$ dBm, respectively. The allowable speed of the UAVs is set to $v_{\max} = 5$ m/s, and the operation altitude of the UAVs is fixed as $H = H_I = H_E = 8$ m.

A. LINEAR EH MODEL

We first focus on the UAV WPCN with the ideal linear EH model configuration. Unless otherwise stated, we adopt a snapshot of uniformly and randomly distributed GTs ($K = 7$) in the area of 120 m \times 120 m, whose locations are marked by squares in Figure 3. We illustrate the optimized trajectories of the UAVs in Figure 3 both for the integrated UAV and the separated UAV WPCNs for $T = 50$ and 110 sec. The circular, triangular, and plus sign markers stand for the positions of UAVs sampled at every 10 sec. First, in Figure 3(a), we can see that the UAV in the integrated UAV WPCN tries to cover all GTs by travelling a path whose center is close to the centroid of the GTs. In contrast, in the separated system, two UAVs mainly cover two different areas so that the ID UAV flies over the upper-right side of the area, while the ET UAV gets around the lower-left side. This is because when $T = 50$ sec, the time period is not enough for two UAVs to visit all the GTs. Therefore, by sectorizing the area, the separated UAV WPCN can transfer energy and receive information more efficiently compared to the integrated WPCN. Note that

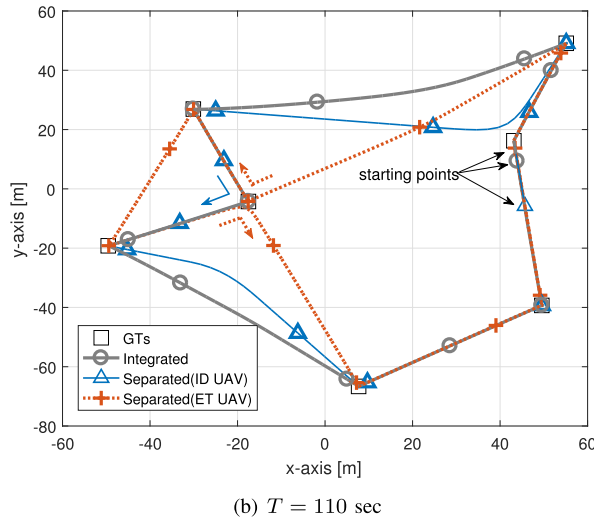
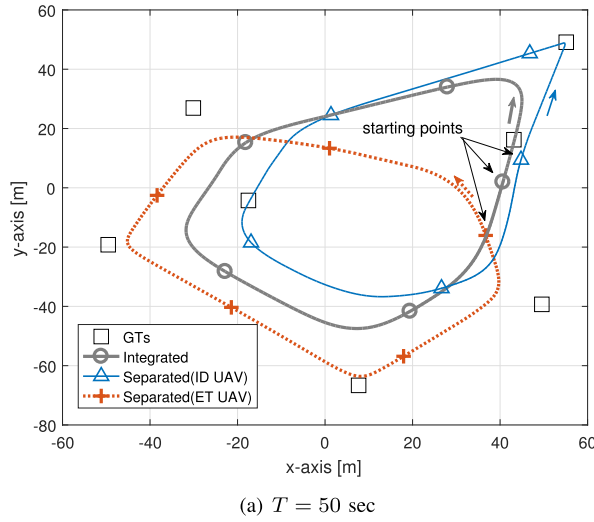


FIGURE 3. Trajectories of UAVs optimized by Algorithm 1.

the minimum throughput performance of the separated UAV WPCN is 28% larger than that of the integrated UAV WPCN for $T = 50$ sec.

From Figure 3(b), it can be seen that the optimized trajectory for the integrated UAV WPCN becomes line segments which connect the locations of the GTs for a large T as in [11]. Nevertheless, the separated UAV WPCN still exhibits non-trivial trajectories where the trajectories of the ID and the ET UAVs are not the same due to the decoupled WET and WIT operations. For $T = 110$ sec, the minimum throughput performance of the separated UAV WPCN is about 16% larger than that of the integrated UAV WPCN.

Figure 4 shows the histogram of the optimized time resource allocation solution of the integrated UAV WPCN for $T = 50$ and 110 sec, which corresponds to Figures 3(a) and 3(b), respectively. We can check that the optimized solution tends to support only a small number of GTs at the same time, which are closely located to the UAV, for efficient uplink WIT. Furthermore, the time fraction assigned for the downlink WET phase decreases as the time

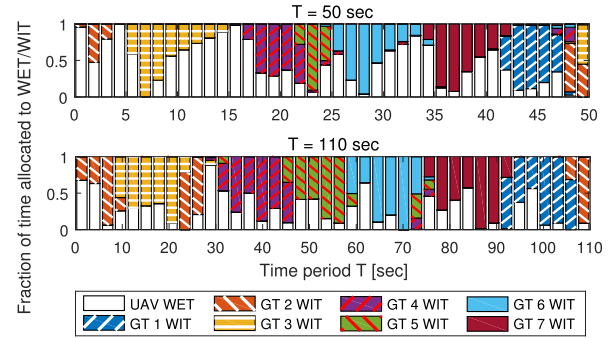


FIGURE 4. Histogram of time resource allocation optimized by Algorithm 1.

period T grows, since there are enough time resources for the UAV to get closer to each GT for decoding the information signal. On the other hands, for a small T , the UAV allocates more time for the WET to charge the GTs to improve the minimum rate performance. As a result, the rate fairness among the GT is well achieved by the optimized UAV trajectories and the time resource allocation solution.

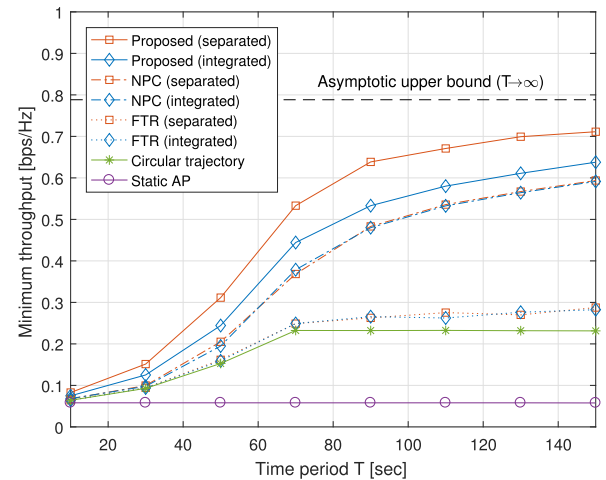


FIGURE 5. Minimum throughput with respect to time interval T for various systems.

Figure 5 illustrates the minimum throughput performance of the proposed algorithms by changing the time period T where the time slot length is set to $\delta_N = 1$ sec. To compare the performance, we also simulate the following baseline schemes.

- **Static AP:** As the conventional static WPCN [22], a fixed H-AP is located at the center of GTs with an altitude of $H = 8$ m. Then the time resource is optimized by the algorithm presented in [22].
- **Circular trajectory:** The UAV trajectory is set to the circular path in [1]. Then, the joint optimization of the uplink power and the time resource in problem (25) is performed for fixed $\{\mathbf{p}[n]\}$. Note that with the circular trajectory, both the integrated UAV and the separated UAV WPCNs achieve the same minimum

rate performance. The circular trajectory is used as an initialization scheme for the proposed algorithms and other baseline schemes.

- *Fixed time resource (FTR)*: With the fixed time resource $\{\tau_k[n]\}$ obtained from the circular scheme, the uplink power and the UAV trajectory are computed by Algorithm 1.
- *Naive power control (NPC)*: With the trajectory and the time resource allocation optimizations based on the proposed algorithms, each GT uses all of the energy harvested at the previous time slot for WIT. If the stored energy at the GT exceeds the uplink power constraint, i.e., $E_k[n-1] > \delta_N \tau_k[n] P_{\max}^{\text{UL}}$, the GT transmits the information signal with P_{\max}^{UL} at the n -th time slot.

From Figure 5, we can check that even when the trajectory is configured as a simple circular path, the minimum throughput performance can be enhanced in comparison with the conventional static WPCN. Also, the FTR case shows a performance enhancement by optimizing the trajectory of the UAV with a simple time resource allocation. These infer that the mobility of the UAV well compensates the doubly near-far problem of the static WPCN. Although the NPC scheme naively controls the uplink power, the minimum throughput is further improved compared to other baseline schemes by jointly optimizing the UAV trajectories and the time resource allocation. The minimum throughput performance of the proposed algorithms increases as the time period T grows, and the performance gap between the proposed algorithm and the asymptotic upper bound of the algorithm with $T \rightarrow \infty$ becomes smaller for a large T . In addition, the performance gap between the proposed schemes and the conventional methods grows with T . Note that this indicates that the optimization of the UAV trajectories and the time resource allocation can bring a huge gain on system performance, and thus these are critical design factors. Moreover, the separated UAV WPCN always performs better than the integrated UAV WPCN in the proposed scheme, while the baseline schemes do not exhibit such advantages. This can be attributed to a fact that in the NPC and the FTR schemes, both the ID and the ET UAV trajectories in the separated system converge to the same trajectory, due to the limited energy causality and time resource allocation. Therefore, we can conclude that jointly optimization of trajectories, uplink power control and time resource allocation is important for the UAV WPCNs.

Figure 6 exhibits the convergence behavior of Algorithm 1 both for the integrated and the separated systems. It is shown that regardless of the time periods T , the proposed algorithm converges to an efficient point within 15 iterations.

B. NON-LINEAR EH MODEL

Now, we investigate the effect of the non-linearity in the EH circuits by evaluating the performance of the proposed algorithm for the non-linear EH model case, i.e., Algorithm 2 in Section IV. We focus on the deployment scenario with $K = 3$

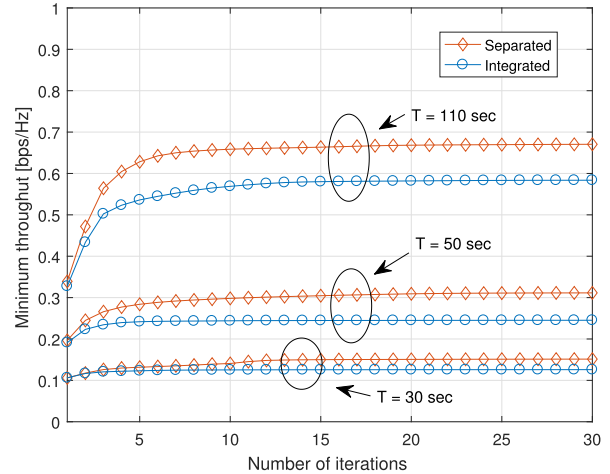


FIGURE 6. Convergence of the proposed Algorithm 1.

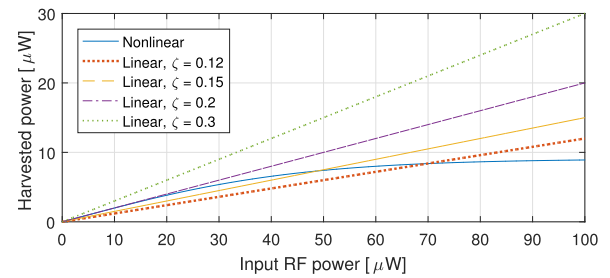


FIGURE 7. Harvested power of the non-linear and the linear EH model with respect to input RF power.

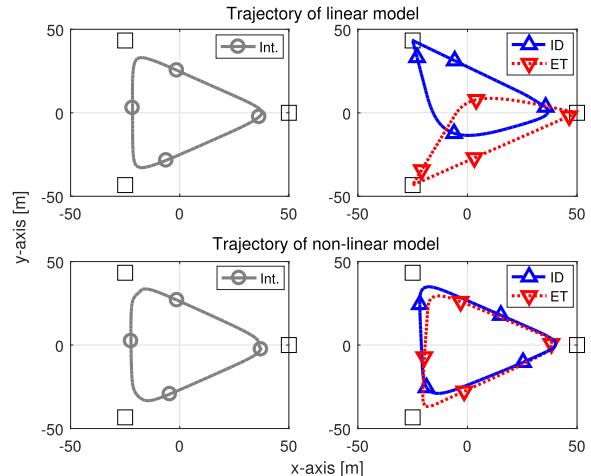


FIGURE 8. Comparison of optimized trajectory between the linear and non-linear EH model systems.

GTs shown in Figure 8 presenting the optimized trajectory for the non-linear EH model with $a = 47083$, $b = 2.9 \times 10^{-6}$, and $M = 9.079 \mu\text{W}$ [21] for the time period of $T = 40$ sec. For comparison, we also depict the trajectory optimized via Algorithm 1 for the linear EH model with $\zeta = 0.2$ which is well-fitted for the non-linear model on the unsaturated region

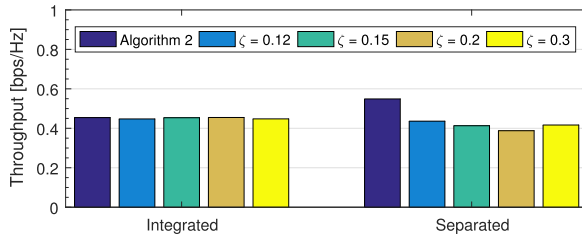


FIGURE 9. Throughput gap between the linear and the non-linear EH model optimization.

as depicted in Figure 7. From Figure 8, we can see that in the integrated UAV systems, the optimized trajectories for the linear and non-linear EH models are almost identical, whereas those in the separated UAV systems are different. To be specific, the ID and the ET UAVs with the linear EH model cover the north and the south parts, respectively. On the contrary, in the practical non-linear EH model scenario, both UAVs try to focus on the central area more compared to the linear model case. This is because the difference of the input-output power characteristic between the non-linear and the linear model illustrated in Figure 7 affects the harvested energy of GTs.

In Figure 9, we illustrate the throughput performance obtained from Algorithm 2. To see the impact of the optimization solution for the non-linear EH model, we also plot the performance of the linear EH model solution of Algorithm 1 applied to the non-linear EH model with $\zeta = \{0.12, 0.15, 0.2, 0.3\}$. It can be shown that in the integrated UAV WPCN, the solution in the linear EH model-based system optimized by Algorithm 1 is close to that of the non-linear EH system. In contrast, in the separated UAV WPCN, Algorithm 2 exhibits better performance for the practical non-linear EH system over Algorithm 1.

VI. CONCLUSION

This paper has studied the UAV-aided WPCN where UAVs perform the WET for the WET of multiple GTs. For both the integrated UAV and the separated UAV WPCNs, the trajectories of the UAVs, the uplink power at the GTs, and the time resource allocation strategies have been jointly optimized for maximizing the minimum throughput among the GTs with the linear and the non-linear EH model. To solve these non-convex problems, we have applied the CCCP for the linear EH system, while the alternating optimization framework and the SCA have been employed for the non-linear EH system. As a result, the efficient solutions of the original non-convex problems have been obtained by the proposed algorithms whose convergence has been mathematically proved. Through the numerical simulations, the efficiency of the proposed algorithms in comparison with the conventional schemes has been demonstrated. As future works, the proposed systems can be further extended to general multi-UAV networks with the association problems of

the GTs and guaranteeing the individual QoS requirement for each GT.

APPENDIX A

PROOF OF PROPOSITION 3

Let us first denote $Z_k[n] = \beta g_0 P^{\text{DL}} / z_k[n]$ and $S_k[n] = \frac{\tau_0[n]M}{\alpha} \left(\frac{1+\alpha}{1+\alpha \exp(-Z_k[n])} - 1 \right)$. Then, the first and the second derivative of $S_k[n]$ with respect to $z_k[n]$ are respectively written as

$$\nabla S_k[n](z_k[n]) = -\tau_0[n] \frac{M(1+\alpha)Z_k[n]^2 \exp(-Z_k[n])}{\beta g_0 P^{\text{DL}} (1+\alpha \exp(-Z_k[n]))^2}, \quad (58)$$

$$\begin{aligned} \nabla^2 S_k[n](z_k[n]) &= \tau_0[n] \frac{M(1+\alpha)Z_k[n]^4 \exp(-Z_k[n])}{(\beta g_0 P^{\text{DL}})^2 (1+\alpha \exp(-Z_k[n]))^2} \\ &\quad \cdot \left(\frac{2}{Z_k[n]} - \frac{1-\alpha \exp(-Z_k[n])}{1+\alpha \exp(-Z_k[n])} \right). \end{aligned} \quad (59)$$

For given $z_k[n] = \hat{z}_k[n]$, a function $E_{k,\text{LB}}^{NL}[n](z|\hat{z}_k[n])$ which is the surrogate function of $S_k[n](z_k[n])$ must satisfy these three conditions [36]

$$S_k[n](\hat{z}_k[n]) = E_{k,\text{LB}}^{NL}[n](\hat{z}_k[n]|\hat{z}_k[n]),$$

$$\nabla S_k[n](\hat{z}_k[n]) = \nabla E_{k,\text{LB}}^{NL}[n](\hat{z}_k[n]|\hat{z}_k[n]),$$

$$S_k[n](z_k[n]) \geq E_{k,\text{LB}}^{NL}[n](z|\hat{z}_k[n]), \quad \forall z \in \mathbb{R}.$$

To meet the conditions, defining $E_{k,\text{LB}}^{NL}[n](z|\hat{z}_k[n])$ as

$$\begin{aligned} E_{k,\text{LB}}^{NL}[n](z|\hat{z}_k[n]) &= S_k[n](\hat{z}_k[n]) + \nabla(S_k[n](\hat{z}_k[n])) \\ &\quad \times (z - \hat{z}_k[n]) + \frac{U_m}{2}(z - \hat{z}_k[n])^2, \end{aligned} \quad (60)$$

where $U(z_k[n]) = -\frac{\tau_0[n]M(1+\alpha)Z_k[n]^4 \exp(-Z_k[n])}{(\beta g_0 P^{\text{DL}})^2 (1+\alpha \exp(-Z_k[n]))^3}$ and $U_m \triangleq \min_{z_k[n] \in \mathcal{U}} U(z_k[n])$. It can be easily shown that $E_{k,\text{LB}}^{NL}[n](z|\hat{z}_k[n])$ in (60) is concave with respect to z and satisfies the first two conditions for the surrogate function. Furthermore, the third condition is also satisfied since $\nabla^2 S_k[n](z_k[n]) \geq U(z_k[n])$ and thus U_m fulfills the Taylor's inequality. Note that thanks to the unimodality of $U(z_k[n])$, U_m can be easily obtained by one-dimensional search algorithms such as the golden-section search method [44]. Finally, by substituting $z = z_k[n]$ in (60) and $\hat{Z}_k[n] = \beta g_0 P^{\text{DL}} / \hat{z}_k[n]$, Proposition 3 is proved.

ACKNOWLEDGMENT

This paper was presented in part at the IEEE VTC2018-Fall, Chicago, USA, August 2018 [1].

REFERENCES

- [1] J. Park, H. Lee, S. Eom, and I. Lee, "Wireless powered communication networks aided by an unmanned aerial vehicle," in *Proc. IEEE Veh. Technol. Conf.*, Chicago, IL, USA, Aug. 2018, pp. 1–5.
- [2] Y. Zeng, R. Zhang, and T. J. Lim, "Wireless communications with unmanned aerial vehicles: Opportunities and challenges," *IEEE Commun. Mag.*, vol. 54, no. 5, pp. 36–42, May 2016.
- [3] N. H. Motlagh, T. Taleb, and O. Arouk, "Low-altitude unmanned aerial vehicles-based Internet of Things services: Comprehensive survey and future perspectives," *IEEE Internet Things J.*, vol. 3, no. 6, pp. 899–922, Dec. 2016.

- [4] P. Zhan, K. Yu, and A. L. Swindlehurst, "Wireless relay communications with unmanned aerial vehicles: Performance and optimization," *IEEE Trans. Aerosp. Electron. Syst.*, vol. 47, no. 3, pp. 2068–2085, Jul. 2011.
- [5] F. Ono, H. Ochiai, and R. Miura, "A wireless relay network based on unmanned aircraft system with rate optimization," *IEEE Trans. Wireless Commun.*, vol. 15, no. 11, pp. 7699–7708, Nov. 2016.
- [6] Y. Zeng, R. Zhang, and T. J. Lim, "Throughput maximization for UAV-enabled mobile relaying systems," *IEEE Trans. Commun.*, vol. 64, no. 12, pp. 4983–4995, Dec. 2016.
- [7] J. Lyu, Y. Zeng, R. Zhang, and T. J. Lim, "Placement optimization of UAV-mounted mobile base stations," *IEEE Commun. Lett.*, vol. 21, no. 3, pp. 604–607, Mar. 2017.
- [8] M. Alzenad, A. El-Keyi, F. Lagum, and H. Yanikomeroglu, "3-D placement of an unmanned aerial vehicle base station (UAV-BS) for energy-efficient maximal coverage," *IEEE Wireless Commun. Lett.*, vol. 6, no. 4, pp. 434–437, Aug. 2017.
- [9] M. M. Azari, F. Rosas, K.-C. Chen, and S. Pollin, "Ultra reliable UAV communication using altitude and cooperation diversity," *IEEE Trans. Commun.*, vol. 66, no. 1, pp. 330–344, Jan. 2018.
- [10] Y. Zeng and R. Zhang, "Energy-efficient UAV communication with trajectory optimization," *IEEE Trans. Wireless Commun.*, vol. 16, no. 6, pp. 3747–3760, Jun. 2017.
- [11] Q. Wu, Y. Zeng, and R. Zhang, "Joint trajectory and communication design for multi-UAV enabled wireless networks," *IEEE Trans. Wireless Commun.*, vol. 17, no. 3, pp. 2109–2121, Mar. 2018.
- [12] M. Chen, M. Mozaffari, W. Saad, C. Yin, M. Debbah, and C. S. Hong, "Caching in the sky: Proactive deployment of cache-enabled unmanned aerial vehicles for optimized quality-of-experience," *IEEE J. Sel. Areas Commun.*, vol. 35, no. 5, pp. 1046–1061, May 2017.
- [13] S. Jeong, O. Simeone, and J. Kang, "Mobile edge computing via a UAV-mounted cloudlet: Optimization of bit allocation and path planning," *IEEE Trans. Veh. Technol.*, vol. 67, no. 3, pp. 2049–2063, Mar. 2018.
- [14] S. ur Rahman, G. Kim, Y. Cho, and A. Khan, "Positioning of UAVs for throughput maximization in software-defined disaster area UAV communication networks," *J. Commun. Netw.*, vol. 20, no. 5, pp. 452–463, Oct. 2018.
- [15] Q. Wu and R. Zhang, "Common throughput maximization in UAV-enabled OFDMA systems with delay consideration," *IEEE Trans. Wireless Commun.*, vol. 66, no. 12, pp. 6614–6627, Dec. 2018.
- [16] R. Zhang and C. K. Ho, "MIMO broadcasting for simultaneous wireless information and power transfer," *IEEE Trans. Wireless Commun.*, vol. 12, no. 5, pp. 1989–2001, May 2013.
- [17] Z. Chen, P. Fan, D. O. Wu, and K. Ben Letaief, "Weighted sum-throughput maximization for MIMO broadcast channel: Energy harvesting with hybrid energy storage," *J. Commun. Netw.*, vol. 19, no. 6, pp. 678–692, Dec. 2017.
- [18] H. Lee, S.-R. Lee, K.-J. Lee, and I. Lee, "Optimal beamforming designs for wireless information and power transfer in MISO interference channels," *IEEE Trans. Wireless Commun.*, vol. 14, no. 9, pp. 4810–4821, Sep. 2015.
- [19] C. Song, J. Park, B. Clerckx, I. Lee, and K.-J. Lee, "Generalized precoder designs based on weighted MMSE criterion for energy harvesting constrained MIMO and multi-user MIMO channels," *IEEE Trans. Wireless Commun.*, vol. 15, no. 12, pp. 7941–7954, Dec. 2016.
- [20] J. Kim, H. Lee, C. Song, T. Oh, and I. Lee, "Sum throughput maximization for multi-user MIMO cognitive wireless powered communication networks," *IEEE Trans. Wireless Commun.*, vol. 16, no. 2, pp. 913–923, Feb. 2017.
- [21] E. Boshkovska, D. W. K. Ng, N. Zlatanov, and R. Schober, "Practical non-linear energy harvesting model and resource allocation for SWIPT systems," *IEEE Commun. Lett.*, vol. 19, no. 12, pp. 2082–2085, Sep. 2015.
- [22] H. Ju and R. Zhang, "Throughput maximization in wireless powered communication networks," *IEEE Trans. Wireless Commun.*, vol. 13, no. 1, pp. 418–428, Jan. 2014.
- [23] L. Liu, R. Zhang, and K.-C. Chua, "Multi-antenna wireless powered communication with energy beamforming," *IEEE Trans. Commun.*, vol. 62, no. 12, pp. 4349–4361, Dec. 2014.
- [24] H. Kim, H. Lee, M. Ahn, H.-B. Kong, and I. Lee, "Joint subcarrier and power allocation methods in full duplex wireless powered communication networks for OFDM systems," *IEEE Trans. Wireless Commun.*, vol. 15, no. 7, pp. 4745–4753, Jul. 2016.
- [25] H. Lee, K. J. Lee, H. B. Kong, and I. Lee, "Sum-rate maximization for multiuser MIMO wireless powered communication networks," *IEEE Trans. Veh. Technol.*, vol. 65, no. 11, pp. 9420–9424, Nov. 2016.
- [26] Y. Shi, L. Xie, Y. T. Hou, and H. D. Sherali, "On renewable sensor networks with wireless energy transfer," in *Proc. IEEE INFOCOM*, Apr. 2011, pp. 1350–1358.
- [27] L. Xie, Y. Shi, Y. Hou, and H. D. Sherali, "Making sensor networks immortal: An energy-renewal approach with wireless power transfer," *IEEE/ACM Trans. Netw.*, vol. 20, no. 6, pp. 1748–1761, Dec. 2012.
- [28] S. Guo, C. Wang, and Y. Yang, "Joint mobile data gathering and energy provisioning in wireless rechargeable sensor networks," *IEEE Trans. Mobile Comput.*, vol. 13, no. 12, pp. 2836–2852, Dec. 2014.
- [29] M. Zhao, J. Li, and Y. Yang, "A framework of joint mobile energy replenishment and data gathering in wireless rechargeable sensor networks," *IEEE Trans. Mobile Comput.*, vol. 13, no. 12, pp. 2689–2705, Dec. 2014.
- [30] T. Li, P. Fan, Z. Chen, and K. B. Letaief, "Optimum transmission policies for energy harvesting sensor networks powered by a mobile control center," *IEEE Trans. Wireless Commun.*, vol. 15, no. 19, pp. 6132–6145, Sep. 2016.
- [31] J. Xu, Y. Zeng, and R. Zhang, "UAV-enabled wireless power transfer: Trajectory design and energy optimization," *IEEE Trans. Wireless Commun.*, vol. 17, no. 8, pp. 5092–5106, Aug. 2018.
- [32] L. Fu, P. Cheng, Y. Gu, J. Chen, and T. He, "Optimal charging in wireless rechargeable sensor networks," *IEEE Trans. Veh. Technol.*, vol. 65, no. 1, pp. 278–291, Jan. 2016.
- [33] J. Xu, Y. Zeng, and R. Zhang, "UAV-enabled wireless power transfer: Trajectory design and energy region characterization," in *Proc. IEEE Globecom Workshops*, Dec. 2017, pp. 1–7.
- [34] Y. Wu, J. Xu, and L. Qiu, "UAV-enabled wireless power transfer with directional antenna: A two-user case," in *Proc. Int. Symp. Wireless Commun. Syst.*, Lisbon, Portugal, Aug. 2018, pp. 1–6.
- [35] L. T. H. An and P. D. Tao, "The DC (difference of convex functions) programming and DCA revisited with DC models of real world nonconvex optimization problems," *Ann. Oper. Res.*, vol. 133, nos. 1–4, pp. 23–46, 2005.
- [36] Y. Sun, P. Babu, and D. P. Palomar, "Majorization-minimization algorithms in signal processing, communications, and machine learning," *IEEE Trans. Signal Process.*, vol. 65, no. 3, pp. 794–816, Feb. 2017.
- [37] M. Razaviyayn, "Successive convex approximation: Analysis and applications," Ph.D. dissertation, Dept. Elect. Eng., Univ. Minnesota, Minneapolis, MN, USA, 2014.
- [38] B. Galkin, J. Kibilda, and L. A. DaSilva, "UAVs as mobile infrastructure: Addressing battery lifetime," *IEEE Commun. Mag.*, vol. 57, no. 6, pp. 132–137, Jun. 2019.
- [39] M. Gatti, F. Giulietti, and M. Turci, "Maximum endurance for battery-powered rotary-wing aircraft," *Aerospace Sci. Technol.*, vol. 45, pp. 174–179, Sep. 2018.
- [40] S. Boyd and L. Vandenberghe, *Convex Optimization*. Cambridge, U.K.: Cambridge Univ. Press, 2004.
- [41] M. Grant and S. Boyd. (2017). *CVX: MATLAB Software for Disciplined Convex Programming*, Version 2.1. [Online]. Available: <http://cvxr.com/cvx>
- [42] Z. Popović, E. A. Falkenstein, D. Costinett, and R. Zane, "Low-power far-field wireless powering for wireless sensors," *Proc. IEEE*, vol. 101, no. 6, pp. 1397–1409, Jun. 2013.
- [43] S. D. Assimonis, S.-N. Daskalakis, and A. Bletsas, "Sensitive and efficient RF harvesting supply for batteryless backscatter sensor networks," *IEEE Trans. Microw. Theory Techn.*, vol. 64, no. 4, pp. 1327–1338, Apr. 2016.
- [44] L. Kiefer, "Sequential minimax search for a maximum," *Proc. Amer. Math. Soc.*, vol. 4, no. 3, pp. 502–506, Jun. 1953.



JUNHEE PARK received the B.S. and M.S. degrees in electrical engineering from Korea University, Seoul, South Korea, in 2015 and 2017, respectively, where he is currently pursuing the Ph.D. degree with the School of Electrical Engineering. His research interests include signal processing and information theory for the next-generation wireless communications, such as UAV-enabled wireless networks and energy harvesting communication systems.



HOON LEE (S'14–M'18) received the B.S. and Ph.D. degrees in electrical engineering from Korea University, Seoul, South Korea, in 2012 and 2017, respectively. In 2015, he visited Imperial College London, London, U.K., to conduct a collaborative research. From 2017 to 2018, he was a Postdoctoral Fellow with Korea University, South Korea, and Singapore University of Technology and Design, Singapore, respectively. Since 2019, he has been with Pukyong National University, Busan, South Korea, where he is currently an Assistant Professor with the Department of Information and Communication Engineering. His research interests include machine learning and signal processing for wireless communications, such as visible light communications, wireless energy transfer communication systems, and secure wireless networks.



INKYU LEE (S'92–M'95–SM'01–F'16) received the B.S. degree (Hons.) in control and instrumentation engineering from Seoul National University, Seoul, South Korea, in 1990, and the M.S. and Ph.D. degrees in electrical engineering from Stanford University, Stanford, CA, USA, in 1992 and 1995, respectively. From 1995 to 2001, he was a member of the Technical Staff with Bell Laboratories, Lucent Technologies, where he studied high-speed wireless system designs. From 2001 to 2002, he was a Distinguished Member of the Technical Staff with Agere Systems (formerly the Microelectronics Group, Lucent Technologies), Murray Hill, NJ, USA. Since 2002, he has been with Korea University, Seoul, where he is currently the Department Head of the School of Electrical Engineering. In 2009, he was a Visiting Professor with the University of Southern California, Los Angeles, CA. He has authored or coauthored more than 180 journal articles in the IEEE publications and holds more than 30 U.S. patents granted or pending. His research interests include digital communications, signal processing, and coding techniques applied for next-generation wireless systems. He was elected as a member of the National Academy of Engineering of Korea, in 2015. He was a recipient of the IT Young Engineer Award from the IEEE/IEEK Joint Award, in 2006, and the Best Paper Award from the Asia-Pacific Conference on Communications, in 2006, the IEEE Vehicular Technology Conference, in 2009, and the IEEE International Symposium on Intelligent Signal Processing and Communication Systems, in 2013. He was also a recipient of the Best Research Award from the Korean Institute of Communications and Information Sciences (KICS), in 2011, the Best Young Engineer Award from the National Academy of Engineering in Korea, in 2013, and the Korea Engineering Award from the National Research Foundation of Korea, in 2017. He has served as an Associate Editor for the IEEE TRANSACTIONS ON COMMUNICATIONS, from 2001 to 2011, and the IEEE TRANSACTIONS ON WIRELESS COMMUNICATIONS, from 2007 to 2011. In addition, he was a Chief Guest Editor for the IEEE JOURNAL ON SELECTED AREAS IN COMMUNICATIONS (Special Issue on 4G Wireless Systems), in 2006. He serves as the Co-Editor-in-Chief for the *Journal of Communications and Networks*. He is an IEEE Distinguished Lecturer.



SUBIN EOM received the B.S. and M.S. degrees in electrical engineering from Korea University, Seoul, South Korea, in 2015 and 2017, respectively, where he is currently pursuing the Ph.D. degree with the School of Electrical Engineering. His research interests include information theory and optimization for the next-generation wireless communications, such as UAV-enabled wireless networks and mobile edge computation networks.